

A General Model for Metal Oxide-Based Memristors and Application in Filters

Valeri Mladenov
Dept. Fundamentals of Electrical
Engineering
Technical University of Sofia
Sofia, Bulgaria
valerim@tu-sofia.bg

Stoyan Kirilov
Dept. Fundamentals of Electrical
Engineering
Technical University of Sofia
Sofia, Bulgaria
s_kirilov@tu-sofia.bg

Ivan Zaykov
Dept. Fundamentals of Electrical
Engineering
Technical University of Sofia
Sofia, Bulgaria
ivanzaykov@tu-sofia.bg

Abstract — Memristors are novel and hopeful electronic memory components. They might be potential substitution of the CMOS elements. Owing to their nano dimensions, low power consumption and memorizing properties, the memristors could be applied in artificial neural networks, memory matrices, programmable analog and digital schemes and other electronic circuits. In this work, a modified and simple, fast operating transition metal oxide-based memristor model is proposed. Its respective LTSPICE library model is created and effectively analyzed in simple memristor-based analog filters. The model's operation is in agreement with the main patterns of the memristive elements. Its correct functioning and applicability in memristor-based electronic circuits is confirmed.

Keywords — memristor model; nonlinear dopant drift; oxide memristors; LTSPICE memristor model; memristor filters

I. INTRODUCTION

The resistance switching in metal oxide-based materials have been investigated since 1970 [1]. Such switching effects are associated to the alteration of the conductance of transition metal oxides in agreement with the voltage and the accumulated charges [1], [2], [3]. These materials might hold their resistance and respective state for a long-time range after turning the electric sources off [3]. They accumulate electric charges, equivalent to the time integral of the flowing current [4], [5]. Therefore, oxides of transition metals as TiO_2 , HfO_2 , Ta_2O_5 , Nb_2O_5 and others could be applied as storing components in memory devices [6], [7]. In 1971 Chua has forecast the fourth basic one-port nonlinear passive electronic element – the memristor [2]. In 2008 the first material sample of a memristor, based on titanium dioxide is created by Hewlett-Packard research team, supervised by Stanley Williams [3]. After this significant discovery, many scientific groups attempted to produce memristors, based on different materials and technologies [8], [9], [10], [11]. Several types memristor components, made of organic and polymeric substances [12], spintronic magnetic systems, amorphous SiO_2 and others are described in the scientific and technical literature. Several of the basic valuable properties of the memristive elements are their non-volatility, memorizing effect, low power consumption, high switching speed, good compatibility to the present CMOS elements, and nano-scale dimensions [13], [14]. These advantageous properties are associated with their potential applications in non-volatile memories, programmable digital and analogue devices, neural nets and other types of electronic circuits [15], [16], [17]. The designing of electronic devices and schemes involves their primary analysis by software simulations [17], [18]. LTSPICE is a very suitable environment for circuit analysis because it is a user-friendly, convenient and free software [18], [19], [20].

The author/s would like to thank the Research and Development Sector at the Technical University of Sofia for the financial support.

Many specific models of TiO_2 , HfO_2 , and Ta_2O_5 memristors are presented in the scientific reports and literature [9], [11]. Due to several specifics of their physical structure and operation in electric field, these memristive elements are quite different [9], [10]. However, in some cases generalized models could be applied for a large class of transition metal oxide-based memristors. Sometimes the specific metal oxide memristor models are relatively complex [13], [15]. The main purpose of this work is to present a simple, fast-functioning and generalized LTSPICE memristor library model, suitable for investigation and simulations of a large group transition metal-oxide memristor elements [3], [11], [15]. The suggested simplified and enhanced memristor model is principally based on both the Lehtonen-Laiho memristor model [13] and the Biolek window function [6]. Its main benefits, according to the existing in the literature memristor models are their simple structure and fast operation at high frequencies. Another advantage of the proposed model is the use of activation (sensitivity) thresholds, which guarantee its applicability in neural networks, programmable analog devices and memory schemes. The suggested memristor model is applied to a tunable analog band-stop filter [20], [21]. After a comparison with experimental current-voltage characteristics of oxide memristors [3], [22] and to results derived by several of the commonly used memristor models, it is established that the suggested model is with a reasonably good accuracy. For limitation of the memristor state variable and representation the boundary effects for hard-switching mode, a modified Biolek window is applied. For avoidance of convergence problems, an improved and differentiable sigmoid function is used in the respective LTSPICE memristor library model.

The rest of the present paper is organized as follows. Section 2 contains a brief description of the transition metal oxide-based memristor elements and their modeling. The proposed general memristor model is expressed in Section 3. The corresponding LTSPICE memristor model is discussed in Section 4. Its application in a simple memristor filter is considered in Section 5. Section 6 concludes the paper.

II. A SUMMARY ON METAL OXIDE MEMRISTORS

For better overview and understanding of the memristor functional operation and their modeling, a brief description of the fundamentals of metal oxide memory elements is first offered. The state variable for TaO_2 and HfO_2 -based memristive elements is presented as a ratio between the lengths of the doped layer w and of those of the complete memristor D [3], [15]. For Ta_2O_5 memristors, the state variable is stated as a ratio between the areas of the conducting region and those of the whole memristor intersection [11]. The state variable x then is: $x = w/D$ [3], [10].

The state-dependent relationship between the memristor voltage v and the current i is [3], [10]:

$$i = M(x)^{-1} \cdot v = [R_{ON}x + R_{OFF}(1-x)]^{-1} \cdot v \quad (1)$$

where (1) is associated with Williams model [3], R_{ON} and R_{OFF} are the ON-state and OFF-state memristances and $M(x)$ is the state-dependent memristance [10]. The equations that completely describe a memristor include the state expression, relating the time derivative of the memristor state variable x and current i , and the current-voltage relation [10]:

$$\begin{cases} x'_t = k i f(x, i) \\ i = M(x)^{-1} \cdot v \end{cases} \quad (2)$$

where $f(x, i)$ is a window function, applied for limitation the memristor state variable x in the interval $[0, 1]$ and for expression of the associated boundary effects, and k is a constant, dependent on the memristor's physical properties – the ionic dopant drift mobility μ , the ON-state resistance R_{ON} and the length of the memristor D [3], [9]:

$$k(v) = \mu(v) \cdot R_{ON} \cdot D^{-2} \quad (3)$$

The dopant drift mobility μ depends on the applied voltage [9]. It grows exponentially if the electric field intensity exceeds a given threshold. The related physical processes in the memristor are extremely complex and could not be accurately described by a simplified model. The simulation time for the standard Biolek model is about 19.3 ms. In order to simplify the model, approximate illustration of the exponential ionic drift is expressed in the following section.

III. THE SUGGESTED GENERALIZED MEMRISTOR MODEL

The proposed modified metal-oxide memristor model is completely described by (4). It is based on Biolek [6] and Lehtonen-Laiho [13] models. The coefficients k_1 and k_2 are parameters for adjustment of the model. The first equation is written according to Biolek model and represents the dependence between the voltage v and the current i . The second and the third equations in (4) are in accordance to Lehtonen-Laiho model and express the time derivative of the variable x as a function of v and i .

$$\begin{cases} v = i \cdot [R_{ON}x + R_{OFF}(1-x)] \\ \frac{dx}{dt} = 0, |v| < v_{thr} \\ \frac{dx}{dt} = k_1 \cdot (k_2 \cdot v)^3 \cdot f_{BM}(x, i), |v| \geq v_{thr} \end{cases} \quad (4)$$

If the level of the applied voltage signal is lesser than the activation threshold v_{thr} , then the memristor operates as a linear resistor and the time derivative of the state variable x is zero. When the voltage is higher than the sensitivity threshold v_{thr} , then the variation of x is proportional to the third power of voltage. The term $(k_2 \cdot v)^3$ is used for approximation of the nonlinear dopant drift [9], [13]. The modified Biolek window $f_{BM}(x, i)$ together with the differentiable sigmoid function $stpp(i)$ are expressed by the next equation set (5) [6], [17]:

$$\begin{cases} f_{BM}(x, i) = 1 - [x - stpp(-i)]^{2p} \\ stpp(i) = 0.5 \cdot [1 + (i^2 + s)^{-0.5} \cdot i] \end{cases} \quad (5)$$

The used window f_{BM} [10], [17] is an enhanced version of the standard Biolek window function [6]. It is founded on the smooth and differentiable function $stpp(i)$, as an alternative of the Heaviside step function. This substitution leads to a partial circumvention of convergence issues in SPICE environment. The constant s determines the sharpness of the function around the switching region. It is in the range scope 0.001 and 0.00001 [10]. The offered metal oxide memristor model is analyzed at sine-wave signals for both soft-switching and hard-switching modes. The best values of the model's coefficients are derived, using parameter estimation, simulation annealing and gradient descent algorithm for minimization of the root mean square error between the simulated and the experimental currents [23], [24]. The optimal values of the parameters are: $k_1 = 2855.4$; $k_2 = 1.0554$; $m = 0.000101$; $x_0 = 0.8544$; $R_{ON} = 132.15$; $R_{OFF} = 1738.24$; $v_{thr} = 0.1054$ V; $p = 9$. The time diagrams of the voltage, state and current, and the current-voltage characteristics are presented in Fig. 1 for comparison and validation of the proper operation of the suggested memristor model. Using (4) and (5) and the derived model's coefficients, the correspondent LTSPICE library model is created.

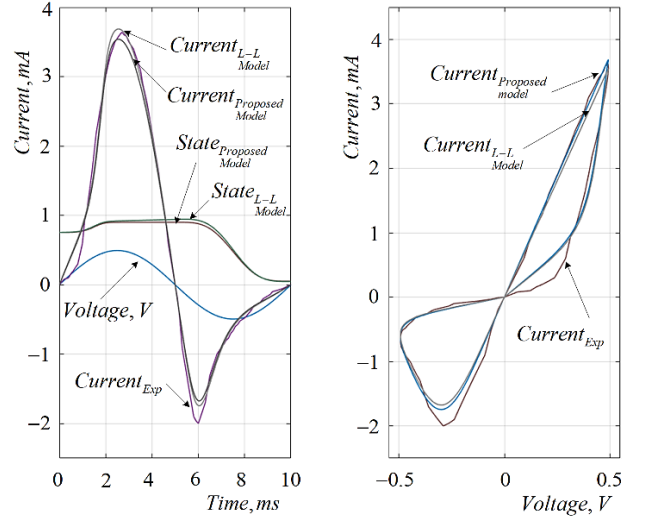


Fig. 1 Time graphs of the memristor voltage, state, experimental and simulated current and the correspondent i - v relations, according to the proposed model and Lehtonen-Laiho memristor model

IV. LTSPICE REALIZATION OF THE MEMRISTOR MODEL

Based on the proposed modified memristor model, described by (5) and (6), LTSPICE memristor library model is generated. The basic elements in the LTSPICE environment are used for the correspondent math operations, according to the suggested memristor model. The equivalent circuit of the generated LTSPICE memristor model is shown in Fig. 2 for supplementary clarifications and discussion. The state variable x is related to the voltage $V(Y)$ across the capacitive element C_1 [10], [17]. Its current is equal to the time derivative of x . The two-port voltage-dependent current source G_2 represents the conductance of the memristor. The internal resistance of the voltage source V_1 is expressed by the resistor R_2 . The resistor R_1 , connected in parallel to the capacitor C_1 defends the scheme from convergence issues [18]. The main terminals of the memristor are the top electrode (te) and the bottom electrode (be). The electrode Y is used for measuring the state variable x [10], [17]. According to the discussed schematic, the correspondent LTSPICE code of the metal oxide-based memristor model is generated and offered below.

```

.subckt A13 te be Y
.params k1=2855.4 k2=1.0554 Ron=132.15 Roff=1738.24
.params Cint=1 pp=9 m=0.000101 vthr=0.1054
Cint Y 0 1 IC=0.8544
R1 Y 0 10G
G1 0 Y value={(k1*(k2*V(te,be))*(k2*V(te,be))*
(k2*V(te,be))*(1-pow((V(Y)-stpp(-V(te,be),m)),(2*pp))))*
(stpp((abs(V(te,be))-vthr),m))}
G2 te be value={V(te,be)/(Ron*V(Y)+Roff*(1-V(Y)))}
.func stpp(x,p)={0.5*(1+(x/sqrt(pow(x,2)+p)))}
.ends A13

```

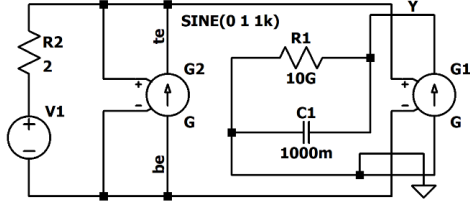


Fig. 2 A schematic of the equivalent LTSPICE memristor model

The schematic used for analysis of the basic characteristics of the suggested memristor model is presented in Fig. 3 for description of the main functional elements. The source B_1 is used for integrating of the memristor voltage and to obtain the correspondent flux linkage [17]. The produced LTSPICE memristor model is investigated by impulse and sine voltage signals with different frequencies.

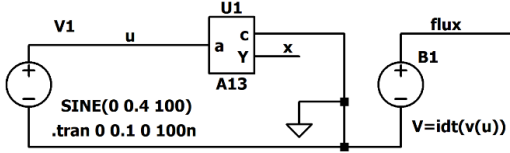


Fig. 3 A schematic of the proposed memristor model for analysis of its basic characteristics – current-voltage and state-flux relationships

The respective current-voltage characteristics are shown in Fig. 4 for establishing of the model's correct operation. It is observable that, if the frequency rises, then the area of the pinched i - v hysteresis loop decreases. This effect is in agreement with the basic patterns of the memristive elements. The correspondent state-flux relationships of the memristor model are presented in Fig. 5 for comparison of their shapes and the change of the state variable. In the first sub-figure, the state-flux characteristic is related to a hard-switching mode, owing to the alteration of the state variable between zero and unity. The other two state-flux relationships correspond to a soft-switching operation.

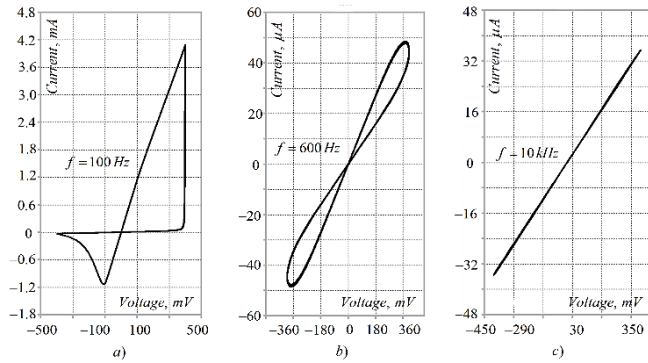


Fig. 4 Current-voltage characteristics of the memristor model, derived for different frequencies: a) $f_1 = 100$ Hz; b) $f_2 = 600$ Hz; c) $f_3 = 10$ kHz

The proposed model is analyzed by pulse operation, properly expressing soft-switching and hard-switching

modes. The simulation time of the offered modified memristor model is about 17.4 ms. With respect to the classical Lehtonen-Laiho model, the discussed memristor model has a higher operating speed. The precision of the proposed model is very close to Lehtonen-Laiho model, according to the error.

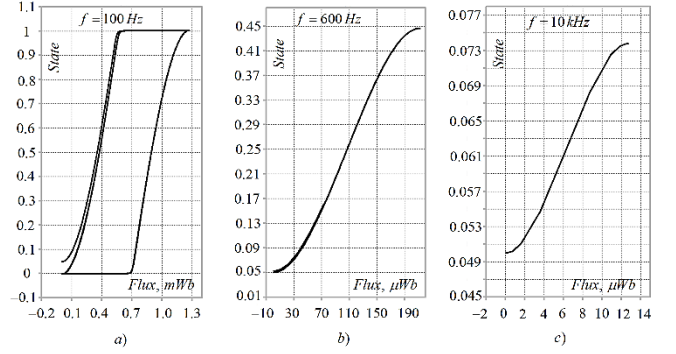


Fig. 5 State-flux relationships of the suggested memristor model, correspondent to the current-voltage characteristics shown in Fig. 4

V. APPLICATION IN A SIMPLE MEMRISTOR FILTER

The described in this section passive band-stop filter is founded on a parallel connection of low-pass and high-pass capacitor-resistor filter modules, where the resistive elements are substituted by memristors. In the considered scheme, the application of inductances is avoided [21]. The filtering circuit is shown in Fig. 6 for additional clarification of its operation and basic properties. The cut-off frequency of the high-pass filtering unit, including the memristor U_1 and the capacitive element C_1 , is higher than the correspondent cut-off frequency of the low-pass filter, based on the memristive element U_2 and the capacitor C_2 [20], [21]. The pass-bands of the low-pass and high-pass filtering groups do not cover one to another. The used memristive model, discussed in the previous sections is denoted by A_{13} . If the capacitor C_1 is directly connected in parallel to the output, then the output voltage becomes zero for higher frequencies, owing to the very low reactance of the capacitor. The resistor R_1 is connected in series with the capacitor C_1 . It prevents the decrease of the output voltage to a zero value for very high frequencies [20], [21].

The amplitude-frequency response of the memristive filter is shown in Fig. 7 for better clarification of its functioning. The resistance of the components U_1 and U_2 is adjusted by external voltage impulses. Thus, the cut-off frequencies and could be altered [21]. The resistive element R_3 guarantees a supplementary current path, and it is used for prevention of convergence issues. The load resistance is with a very high value. The resistor R_2 is applied for altering the output signal level for the higher frequencies [19], [20].

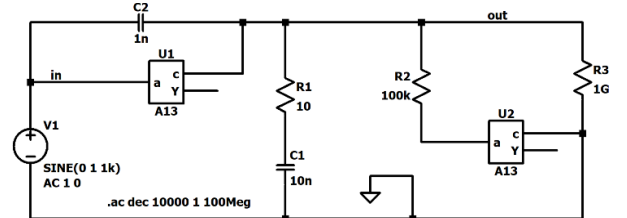


Fig. 6 A schematic of a simple band-stop memristor-based filtering circuit

The cut-off frequency of the memristor low pass filtering module of the designated band-stop filter depends on the memristance M and the capacity C_1 [19], [21]:

$$f_{cut-off\ low} = (2\pi C_1 M_1)^{-1} \quad (6)$$

The respective cut-off frequency of the high pass group is expressed as follows [19], [20]:

$$f_{\text{cut-off high}} = (2\pi C_2 M_2)^{-1} \quad (7)$$

The stop frequency band of the band-stop filter is a difference between the cut-off frequencies [19], [20], [21]:

$$\Delta f_{\text{pass}}(M_1, M_2) = f_{\text{cut-off high}} - f_{\text{cut-off low}} \quad (8)$$

The alteration of the stop frequency band is derived by the change of the memristor state variable, applying external positive or negative voltage pulses [21].

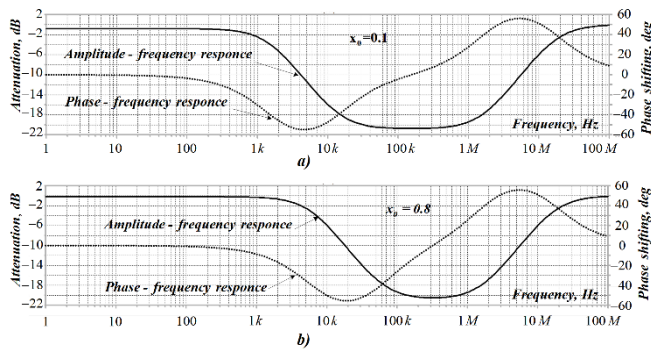


Fig. 7 Amplitude-frequency response and phase-frequency response of the memristor filter for a) initial value of the state variable $x_0 = 0.1$; b) $x_0 = 0.8$

VI. CONCLUSION

The proposed altered and enhanced metal oxide memristor model is mainly based on the standard Williams and Lehtonen-Laiho models, with a modified and highly nonlinear dependence between the time derivative of the state variable and the voltage. It allows the model to properly operate at higher frequencies. Based on the described metal oxide memristor model, denoted by A_{13} , a band-stop filter is analyzed and its functioning is illustrated, paying attention on its basic advantages, according to its classical resistor-capacitor alternative. The correct operation of the proposed model is approved by comparison with some standard existing memristor models, as these of Joglekar, Biolek and Lehtonen-Laiho. Owing to the use of sensitivity threshold, the described modified memristive model is effectively applied in a reconfigurable memristor-based passive band-stop filter. In the typical operating mode of the filtering device, if the memristor voltage is lesser than the sensitivity threshold, then the resistance of the memristor element is a constant and the filter acts as a linear circuit. For altering the cut-off frequencies and the respective stop frequency band of the scheme, external voltage impulses are applied to the memristive element for tuning its resistance. Though for high frequency signals Joglekar and Biolek models are capable to correctly operate in the filtering circuit, the proposed model A_{13} performs better, rendering to the linearity of the filter scheme, due to the use of activation thresholds.

REFERENCES

- [1] Chiu, F.C. „A Review on Conduction Mechanisms in Dielectric Films,” *In Advanced Materials Science Engineering*, Hindawi Publishing Corporation: London, UK, 2014, Vol. 2014, pp. 1–18.
- [2] Chua, L. „Memristor-The missing circuit element,” *IEEE Transactions on Circuit Theory*, 1971, 18, pp. 507–519.

- [3] Strukov, D.B., Snider, G.S., Stewart, D.R., Williams, S., „The missing memristor found,” *Nature* 2008, 453, pp. 80–83.
- [4] Baker, M., Jaoude, A., Kumar, V., Al Homouz, D., Nahla, Heba, A., Al-Qutayri, M., Christoforou, N., "State of the art of metal oxide memristor devices," *Nanotechnology Reviews*, vol. 5, no. 3, doi: 10.1515/ntrev-2015-0029, 2016, pp. 311–329.
- [5] Joglekar, Y., Wolf, S. J. "The elusive memristor: Properties of basic electrical circuits," *Eur. J. Phys.* 2009, 30, pp. 661–675.
- [6] Biolek, Z., Biolek, D., Biolkova, V., "SPICE Model of Memristor with Nonlinear Dopant Drift," *Radioengineering* 2009, 18, pp. 210–214.
- [7] Linn, E., Siemon, A., Waser, R., Menzel, S., "Applicability of Well-Established Memristive Models for Simulations of Resistive Switching Devices," *IEEE Trans. Circuits Syst.* 2014, 61, pp. 2402–2410.
- [8] Corinto, F., Ascoli, A., "A Boundary Condition-Based Approach to the Modeling of Memristor Nanostructures," *IEEE Transactions on Circuits and Systems* 2012, 59, pp. 2713–2727.
- [9] Strukov, D.B., Williams, R.S., "Exponential ionic drift: Fast switching and low volatility of thin-film memristors," *Applied Physics A* 2009, 94, pp. 515–519.
- [10] Ascoli, A., Corinto, F., Senger, V., Tetzlaff, R., "Memristor Model Comparison," *IEEE Circuits Syst. Mag.* 2013, 13, pp. 89–105.
- [11] Strachan, J., Torrezan, A., Miao, F., Pickett, M., Yang, J., Yi, W., Medeiros-Ribeiro, G., Williams, R.S., "State Dynamics and Modeling of Tantalum Oxide Memristors," *IEEE Transactions on Electron Devices* 2013, 60, pp. 2194–2202.
- [12] Chen, Y., Liu, G., Wang, C., Zhang, W., Li, R.-W., Wang, L., "Polymer memristor for information storage and neuromorphic applications," *Mater. Horizons* 2014, 1, pp. 489–506.
- [13] Lehtonen, E., Laiho, M., "CNN using memristors for neighborhood connections," *In Proceedings of the 2010 12th International Workshop on Cellular Nanoscale Networks and their Applications (CNNA 2010)*, Berkeley, CA, USA, 3–5 February 2010, pp. 1–4.
- [14] Mladenov, V., "Advanced Memristor Modeling—Memristor Circuits and Networks," *MDPI: Basel, Switzerland*, 2019, ISBN 978-3-03897-104-7 (Hbk), pp. 172.
- [15] Amer, S., Sayyaparaju, S., Rose, G.S., Beckmann, K., Cady, N.C., "A practical hafnium-oxide memristor model suitable for circuit design and simulation," *In 2017 IEEE International Symposium on Circuits and Systems (ISCAS)* 2017 May 28, pp. 1–4.
- [16] Solovyeva, E. B., Azarov, V. A., "Comparative Analysis of Memristor Models with a Window Function Described in LTspice," *2021 IEEE Conference of Russian Young Researchers in Electrical and Electronic Engineering (ElConRus)*, 2021, pp. 1097–1101.
- [17] Mladenov, V., "A Unified and Open LTSPICE Memristor Model Library," *MDPI Electronics*, 2021, Vol. 10, no. 13: 1594. <https://doi.org/10.3390/electronics10131594>.
- [18] Yang, Y., Lee, S.C. "Circuit Systems with MATLAB and PSpice"; *John Wiley & Sons: Hoboken, NJ, USA*, 2008, ISBN 978-04-7082-240-1, pp. 532.
- [19] Winder, S., "Analog and digital filter design," 2002, *Elsevier Science, USA*, ISBN 0-7506-7547-0.
- [20] Lautaro Fernandez-Canque, H., "Analog Electronics Applications – fundamentals of design and analysis," *CRC Press Taylor & Francis Group*, ISBN 978-1-4987-1495-2, 2017.
- [21] Kirilov, S., Yordanov, R., Mladenov, V., "Analysis and Synthesis of Band-Pass and Notch Memristor Filters," *WSEAS Recent Advances in Telecommunications and Circuit Design*, ISBN: 978-960-474-310-0, pp. 74 – 77.
- [22] Ghedira, S., Rziga, F. O., Mbarek, K., Besbes, K., "Coexistence of Bipolar and Unipolar Memristor Switching Behavior," *In Memristors - Circuits and Applications of Memristor Devices*. London, United Kingdom: IntechOpen, 2019, doi: 10.5772/intechopen.85176.
- [23] Carrillo M., González, José M., "A new approach to modelling sigmoidal curves," *Technological Forecasting and Social Change*, Vol. 69, Issue 3, 2002, ISSN 0040-1625, pp. 233–241.
- [24] Chen S., Billings S., Luo W., "Orthogonal least squares methods and their application to non-linear system identification," *International Journal of Control*, Taylor & Francis, 1989, <https://doi.org/10.1080/00207178908953472>, pp. 1873 - 1896.